

# Delamination of a composite laminated under monotonic loading

Habib Achache<sup>\*1</sup>, Abdelouahab Benzerdjeb<sup>2a</sup>, Abdelkader Mehidi<sup>3a</sup>, Benali Boutabout<sup>3b</sup>  
and Djamel Ouinas<sup>4b</sup>

<sup>1</sup>Department of Materials Engineering, University Dr Yahia Fares of Medea, Urban Pole - 26000 Medea, Algeria

<sup>2</sup>Department of Mechanical Engineering University of Science and Technology Oran Mohammed Boudiaf (USTO),  
BP1505 El Menaouar, 31036 Oran, Algeria

<sup>3</sup>Laboratory of Mechanical and Physical of Materials (LMPM), University Djillali Liabes of Sidi Bel Abbes,  
BP 89, Street Ben M'Hidi, Sidi Bel Abbes, Algeria

<sup>4</sup>Laboratory of Numerical and Experimental Modeling of Mechanical Phenomena, University of Mostaganem,  
Route Belahcel 27000 Mostaganem, Algeria

(Received December 12, 2016, Revised May 4, 2017, Accepted May 5, 2017)

**Abstract.** Our work aims to analyze using the finite element method the evolution of the stress intensity factor (SIF) parameter K of three laminated folded plates stacks  $[+\alpha, -\alpha]$ , made of the same epoxy matrix and different reinforcement fibers (boron, graphite and glass). Our results show that the angle of orientation of the boron/epoxy composite has no great influence on the variation of the parameter KI. Compared to composite graphite/epoxy and glass/epoxy, the laminated composite boron/epoxy reduces more the SIF KI in the middle of the plate for angles  $0^\circ \leq \alpha \leq 30^\circ$ .

**Keywords:** cracks; delamination; stress intensity factor; fibers orientations; finite element method and laminates

## 1. Introduction

The use of long-fiber laminates and organic matrix (O.M.C) continues to grow in most of various fields of engineering applications. The good specific mechanical properties of these materials make it possible to relief structures, particularly in the aeronautical and aerospace industries. Although these materials have several advantages, they should be used with caution.

Damage mechanisms involved in laminated composites are contrary to that of conventional metallic materials. One of the most important types of deterioration encountered in laminated composite materials is the decomposition of the two layers. This damage is known as delamination, which can be observed according to the scale of study. The resistance of the material decreases significantly due to delamination.

Practically, it is very important to identify the initiation of delamination and prevent further spread resulting in ultimate failure (Maimi *et al.* 2011). In addition, the prediction for the beginning of the delamination is also useful for the structure design. (Short *et al.* 2001) have studied the effect of the geometry and location of a single square delamination. The results of their experiments and finite element analyzes show that the size of the delamination and position through the thickness, affects the compression breaking load. (Kutlu and Chang 1992)

reported the first studies on the effects of delamination on the compression behavior of multiple laminates (one or two). They performed an analytical and experimental analysis to determine the effects of the size and position across the width of delamination. (Wang *et al.* 2005) studied the effects of single and multiple position delamination on compressive resistance of the composite reinforced with glass fiber. Their experimental and numerical results show that several delaminations reduce the compressive resistance more than one delamination. (Li *et al.* 2015) used a LayerWise method to study the effects of the size and position of several delamination for unidirectional and diagonal beams. (Suemasu *et al.* 2008) determines the behavior in compression and composite failure mechanism with several circular delaminations using cohesive interface elements. Their results indicate that the load capacity of a composite structure with several delaminations depends on the growth of delamination (Suemasu *et al.* 2008). (Jayatilake *et al.* 2016) have developed a 3D finite element model to study the dynamic behavior (free vibration) of multilayer composite sandwich panels with delaminated interlayer. The results suggest that the size of delamination and the boundary conditions are the main factors responsible for the reduction in stiffness due to damage in composite laminates (Jayatilake *et al.* 2016). A survey was Conducted again by TODO *et al.* using the model and fashion II ENF (End Notched Flexure) composite glass-fiber/vinyl ester (Todo *et al.* 2000). Haneef *et al.* (2011) have carried out finite element analysis to analyze the delamination effect on composite structures with two models (Haneef *et al.* 2011). TODO and JAR presented a finite element study on micro-macro mechanical growth of interlaminar crack array fiberglass/epoxy DCB specimens for mode I (Todo and Jar 1998). Liu *et al.* (2015) studied

\*Corresponding author, Ph.D.

E-mail: [achachehabib@yahoo.fr](mailto:achachehabib@yahoo.fr)

<sup>a</sup>Ph.D.

<sup>b</sup>Professor

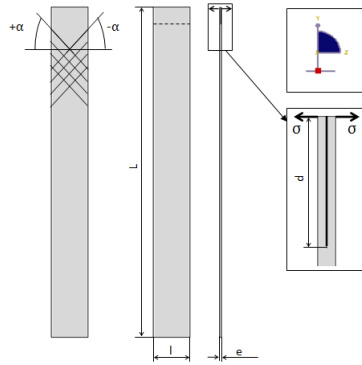


Fig. 1 Geometric model

$l$ : width of the plate=20 mm

$L$ : Length of the laminate sheet=150 mm

$e$ : plate thickness=1 mm (8 plies)

$d$ : Length of variable delamination (30 to 60) mm

$\alpha$ : fiber orientation angle ( $+\alpha -\alpha$ )

$\sigma$ : variable applied stress (1 to 10) MPa

the mechanical behavior of curved laminates experimentally and numerically using three right angle composite angles to determine progressive failure modes based on the Ye criterion of resistance failure. They found that the mode of failure of all specimens is delamination. Liu *et al.* (2015) developed an analytical model to study the effect of a crack of the edge on the characteristics of vibration of the delaminated beams.

The present work aim is to analysis, by the finite element method, the evolution of the stress intensity factor parameter  $K$  of three laminated folded plates stacks [ $+\alpha$ ,  $-\alpha$ ], made of the same epoxy matrix and various reinforcing fibers (boron, graphite and glass), by varying several parameters such as the fiber orientation, the delamination length and the load applied.

## 2. Geometric model

Our model is an orthotropic square plate of  $150 \times 20$  mm<sup>2</sup> consisting of eight 0.125 mm thick crossed plies [ $+\alpha$ ,  $-\alpha$ ]; each layer with an epoxy matrix is reinforced by glass or graphite or bore fibers Fig. 1.

The material mechanical properties of the unidirectional composites are shown in Table1 (Seo and Lee 2002).

The Simulation of linear tensile behavior and the influence of fiber orientation and other parameters, have been carried out using the numerical code Abaqus (Abaqus Standard Version 6.12.2012) and this for the analysis of composite structures was done by the finite element method. This code provides a complete system,

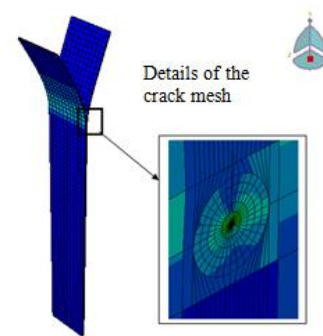


Fig. 2 Mesh with quadrilateral elements of quadratic type

incorporating not only the actual computing functions, but also the model construction functions (preprocessor) and output treatment (post-processor). To properly conduct this study, we have chosen a three-dimensional element whose quadrilateral elements are of quadratic type (see Fig. 2).

## 3. Theory and results

### 3.1 Theory

The stress intensity factor,  $K$  is used in fracture mechanics to predict the stress state (“stress intensity”) near the tip of a crack caused by a remote load or residual stresses (Anderson 2005). It is a theoretical construct usually applied to a homogeneous, linear elastic material and is useful for providing a failure criterion for brittle materials. The concept can also be applied to materials that exhibit *small-scale yielding* at a crack tip.

The magnitude of  $K$  depends on sample geometry, the size and location of the crack, and the magnitude and the modal distribution of loads on the material.

Linear elastic theory predicts that the stress distribution ( $\sigma_{ij}$ ) near the crack tip, in polar coordinates ( $r, \theta$ ) with origin at the crack tip, has the following form (Tada *et al.* 2000).

$$\sigma_{ij}(r, \theta) = \frac{K}{\sqrt{2\pi r}} f_{ij}(\theta) + \text{higher.order.terms} \quad (1)$$

Where:

$\sigma_{ij}$  is the stress as a function of the polar coordinates

$K$  is the stress intensity factor (with units of stress $\times$ length<sup>1/2</sup>),

$f_{ij}$  is a dimensionless quantity that depends on the load and geometry

This relation breaks down very close to the tip (small  $r$ ) because as  $r$  goes to 0, the stress  $\sigma_{ij}$  goes to  $\infty$ . Plastic distortion typically occurs at high stresses and the linear elastic solution is no longer applicable close to the crack tip.

Table 1 Mechanical properties of composites

Proprieties	E11 [MPa]	E22 [MPa]	E33 [MPa]	$\nu_{12}$	$\nu_{13}$	$\nu_{23}$	$G_{12}$ [MPa]	$G_{13}$ [MPa]	$G_{23}$ [MPa]
Glass/epoxy	50000	14500	14500	0.33	0.33	0.33	2560	2560	2240
Boron/epoxy	208000	25400	25400	0.1677	0.1677	0.035	7200	7200	4900
Graphite/epoxy	13400	10300	10300	0.33	0.33	0.53	5500	5500	3200

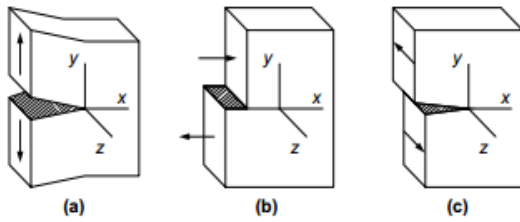


Fig. 3.1 Schematic of the basic fracture modes: (a) Mode I (opening), (b) Mode II (sliding), (c) Mode III (tearing)

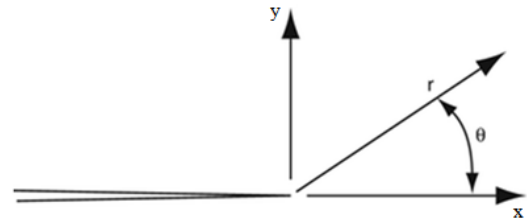


Fig. 3.2 Crack tip coordinate system (Stress Intensity Factors)

However, if the crack-tip plastic zone is small, it can be assumed that the stress distribution near the crack is still given by the above relation.

3.1.1 Stress intensity factors for various modes

Three linearly independent cracking modes are used in fracture mechanics. These load types are categorized as mode I, II, and III (Fig. 3.1 (a), (b) and (c)). Mode I is an opening (tensile) mode where the crack surfaces move directly apart. Mode II is a sliding (in-plane shear) mode where the crack surfaces slide over one another in a direction perpendicular to the leading edge of the crack. Mode III is a tearing (antiplane shear) mode where the crack surfaces move relative to one another and parallel to the leading edge of the crack. Mode I is the most common load type encountered in engineering design.

Different subscripts are used to designate the stress intensity factor for the three different modes. The stress intensity factor for mode I is designated  $K_I$  and applied to the crack opening mode. The mode II stress intensity factor,  $K_{II}$ , applies to the crack sliding mode and the mode III stress intensity factor,  $K_{III}$ , applies to the tearing mode. These factors are formally defined as (Rooke and Cartwright 1976).

$$K_I = \lim_{n \rightarrow \infty} \sqrt{2\pi r} \cdot \sigma_{yy}(r, \theta) \quad (2)$$

Where:

- $K_I$  is the stress intensity factor for mode I
- $\sigma_{yy}$  is the stress as a function of the polar coordinates

The Crack tip coordinate system (Stress Intensity Factors) is shown in Fig. 3.2.

3.2 Results

3.2.1 Influence of the width of delamination on stress intensity factors of three composite

Fig. 4 shows the variation of the stress intensity factors  $K_I$ ,  $K_{II}$  and  $K_{III}$  depending on the width of delamination of glass / epoxy composite. It is noted that the delamination spread of the composite plate is carried out in pure mode I and this according to the force applied to the composite.  $K_I$  stress intensity factor is much higher than the other two failure modes according to the plan and the anti-slip map, which shows that the detachment of the folds happens in pure mode I. In our study the pure mode I is predominant and it is the only parameter to be considered and the two sliding modes  $K_{II}$  and  $K_{III}$  are neglected.

3.2.2 Influence of the width of delamination of the composite glass/epoxy on the  $K_I/K_{IC}$  ratio for different angles  $\alpha$  ( $+\alpha/-\alpha$ ) and different lengths "d"

Fig. 5 shows the variation of ratio  $K_I/K_{IC}$  ratio as a function of the delamination width for different angles of orientation  $+\alpha/-\alpha$  of the folds of the glass/epoxy composite and different lengths d of the detached surface. The graphs of Figs. 5(a), 5(b), 5(c), 5(d), 5(e), 5(f) and 5(g) are respectively determined for the delamination lengths 30 mm, 35 mm, 40 mm, 45 mm, 50 mm, 55 mm and 60 mm. It should be noted that regardless of the length of detachment of the layers of the glass/epoxy laminate composite, the curve of the ratio  $K_I/K_{IC}$  has a symmetry with respect to the middle of the delamination width and therefore the analysis could be performed over half the width of delamination. From the numerical results obtained by the finite element

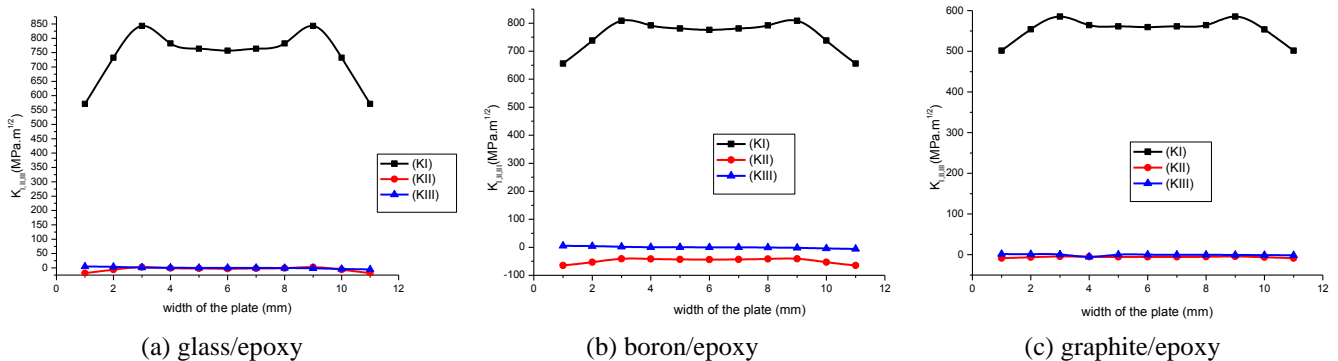


Fig. 4 Variation of the stress intensity factors  $K_I$ ,  $K_{II}$  and  $K_{III}$  depending on the width of delamination of the three composites for  $\alpha=0^\circ$  and  $d=30$  mm

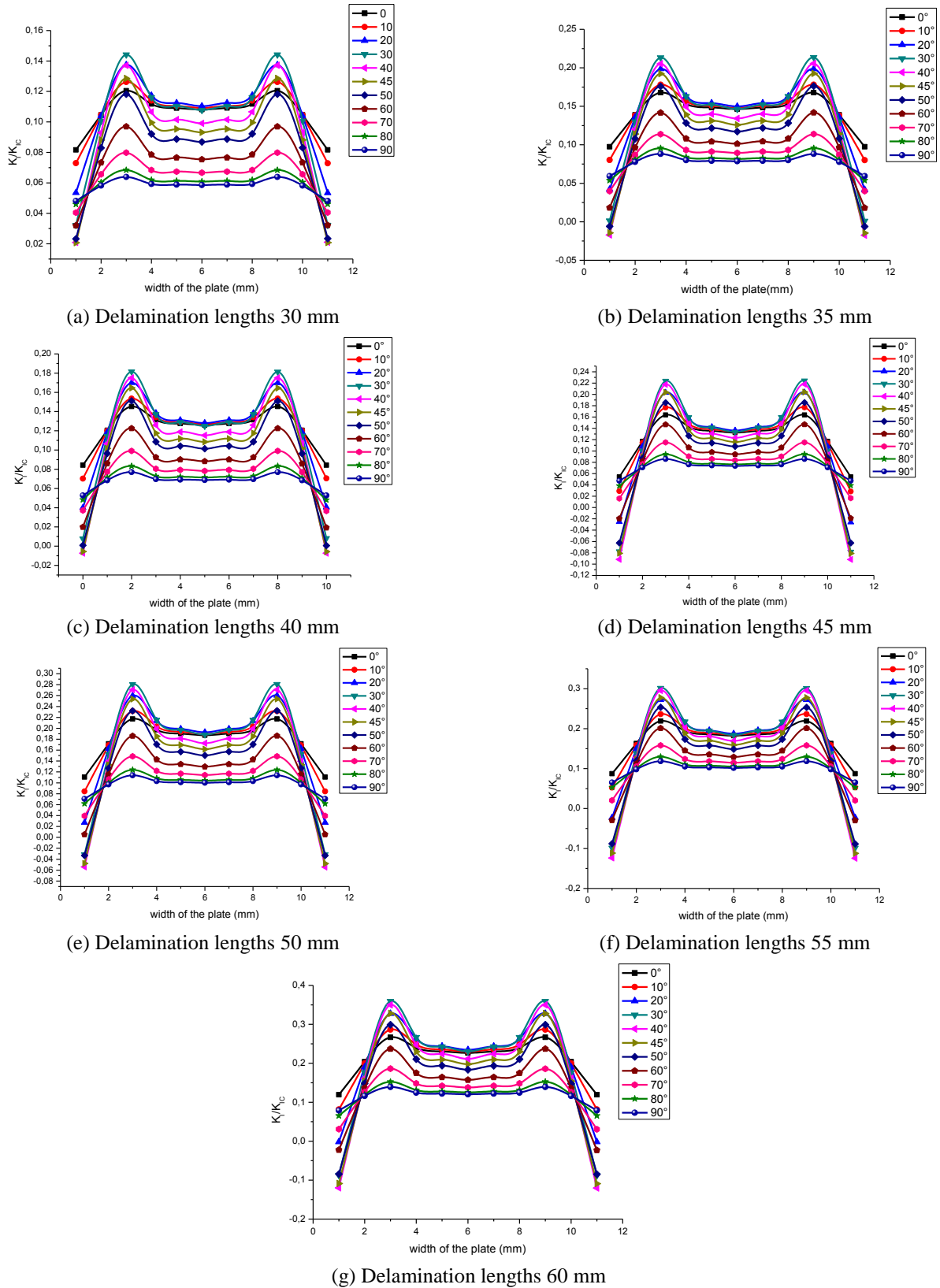


Fig. 5 Variation of  $K_I/K_{Ic}$  depending on the width of delamination of the composite glass/epoxy for different angles  $\alpha$  ( $+\alpha/-\alpha$ ) and different lengths (a: 30 mm b: 35 mm c: 40 mm, d: 45 mm, e: 50 mm f: 55 mm, g: 60 mm)

method, there are three different zones of the curve of the ratio  $K_I/K_{Ic}$ :

The first zone is located at the free edges of the

composite plate over a distance of 10% of the delamination half width in which the value of  $K_I/K_{Ic}$  ratio depends on the angle  $\alpha$  of the layers of the laminated composite and the

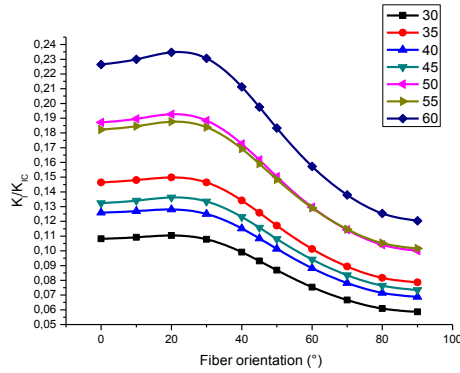


Fig. 6 variation of the  $K_I/K_{IC}$  ratio in the middle of the composite plate as a function of the angle  $\alpha$  for different lengths  $L$  of the detachment surface

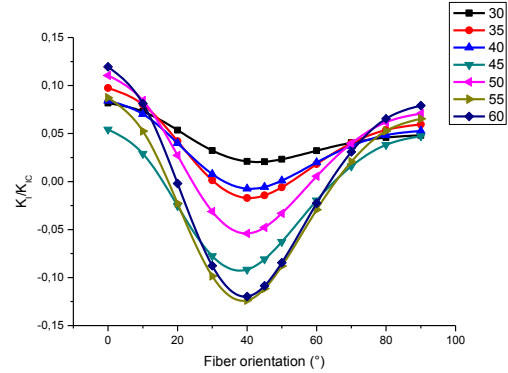


Fig. 7 Variation of the  $K_I/K_{IC}$  ratio to the free edge of the composite plate as a function of the angle  $\alpha$  of the glass/epoxy for different lengths  $d$  of the detachment surface.

surface of detachment and it reaches minimum values in this area and even negative values. At the free edges of the composite, it can be seen that regardless of the angle  $\alpha$  and the length  $d$  of the detachment surface, the propagation of the delamination is either slowed down or completely stopped.

The second zone is in the vicinity close to the free ends over a distance of 20% of the half width of the detachment. It is noted that regardless of the angle  $\alpha$  and the length  $L$  the curve of the ratio  $K_I/K_{IC}$  is in the form of a parabola, it increases progressively to reach a peak and then decreases to a stable value in the middle of the plate composite. It is noted that the peak of the stress intensity factor is more intense for the angles of orientations of the fibers ranging from  $0^\circ$  to  $50^\circ$  and its intensity decreases with the increase of the angle  $\alpha$  in the interval  $[60^\circ, 90^\circ]$ . The two orientations of the fibers at the  $80^\circ$  and  $90^\circ$  angles result in a small peak of the SIF  $K_I$ . It is also observed that the increase in the detachment surface leads to an increase in the peak of the SIF  $K_I$ .

The third zone is in the middle of the composite plate over a distance of 20% of the half width of delamination. It can be seen that, regardless of the angle  $\alpha$  and the length  $L$ , the  $K_I/K_{IC}$  ratio is almost constant and the level of the stress intensity factor  $K_I$  depends strongly on the angle of orientation of the fibers and the length of delamination.

### 3.2.3 Influence of fiber orientation on the $K_I/K_{IC}$ ratio in the middle of the plate

Fig. 6 illustrates the variation of the  $K_I/K_{IC}$  ratio in the middle of the composite plate as a function of the angle  $\alpha$  for different lengths  $d$  of the detachment surface. It should be noted that whatever the length  $d$ , the ratio  $K_I/K_{IC}$  is almost constant for angles  $\alpha$  ranging from  $0^\circ$  to  $30^\circ$  and then decreases proportionally to the angle of orientation of the folds to a minimum value corresponding to  $\alpha=90^\circ$ .

### 3.2.4 Influence of fiber orientation on the $K_I/K_{IC}$ ratio at the free edge of the plate

Fig. 7 illustrates the variation of the  $K_I/K_{IC}$  ratio at the free edge of the composite plate as a function of the angle  $\alpha$  for different lengths  $d$  of the detachment surface. It can be

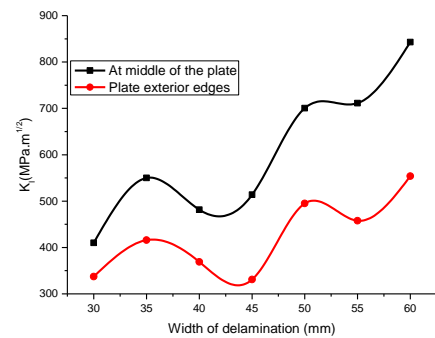


Fig. 8 Variation of the FIC  $K_I$  as a function of the delamination length for different positions (middle and outer) with  $\alpha=90^\circ$

seen that the curve of the parameter  $K_I/K_{IC}$  is in the form of a parabola whose extremum corresponds to the angle  $\alpha=40^\circ$  for the different lengths of delamination. It is also noted that the variation of  $K_I/K_{IC}$  is not proportional to the detachment surface, confirming the results obtained previously (see Fig. 6).

### 3.2.5 Influence the length of delamination on factor $K_I$

Fig. 8 shows the variation of the SIF  $K_I$  as a function of the delamination length for an angle  $\alpha=90^\circ$ , this curve shows the effect of the length of the detachment surface on the parameter  $K_I$ . From the results obtained numerically, it is noted on one hand that the parameter  $K_I$  increases with the increase of delamination the length and on the other hand this variation is not proportional to this length.

### 3.2.6 Influence of the mechanical properties of the composite on the parameter $K_I$

Fig. 9 illustrates the variation of the SIF  $K_I$  as a function of the delamination width for the three glass/epoxy, graphite/epoxy and boron/epoxy laminated composites. These graphs are determined for a detachment length equal to 30 mm and the angles of orientations of the folds ranging from  $0^\circ$  to  $90^\circ$  with a pitch of  $10^\circ$  and they show the influence of the mechanical properties of the composite on the parameter  $K_I$ . It is noted that the SIF  $K_I$  is almost constant along the delamination width of the composite

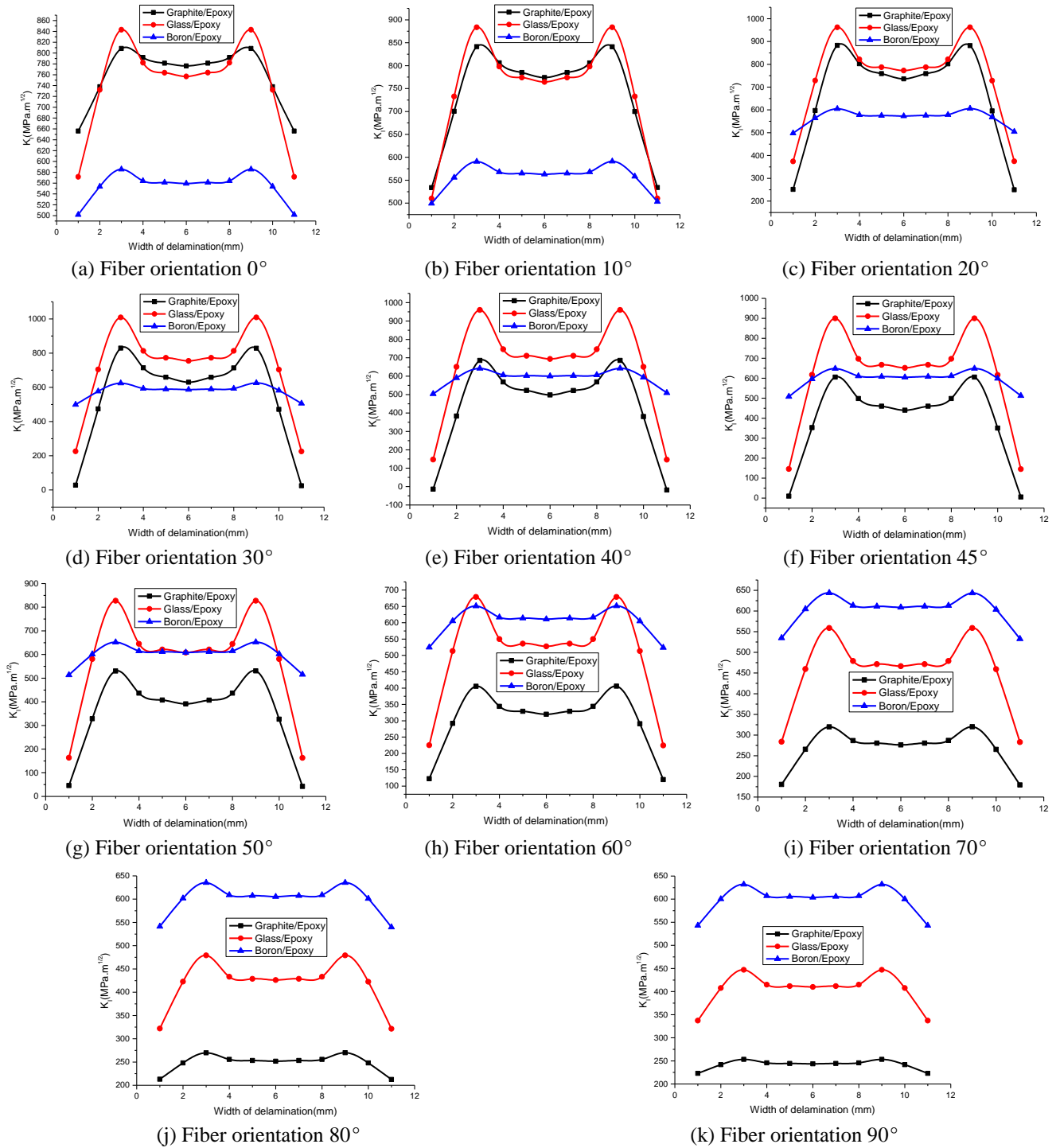


Fig. 9 Variation of the  $K_I$  factor as a function of the width of delamination of composites (glass/epoxy, graphite/epoxy and boron/epoxy) for different angles  $\alpha$  ( $+\alpha/-\alpha$ ) (has a: 0°, b: 10°, c: 20°, d: 30°, e: 40°, f: 45°, g: 50°, h: 60°, i: 70°, j: 80° and k: 90°)

plate with the presence of a slight variation at the free ends of the boron/epoxy composite, whatever the angle  $\alpha$  of the fibers. Consequently, for this type of composite, the angle of orientation of the fibers does not have a great influence on the variation of the parameter  $K_I$ . Compared to graphite/epoxy and glass/epoxy composites, the boron/epoxy laminate composite further reduces the SIF  $K_I$  in the middle of the plate for angles  $0^\circ \leq \alpha \leq 30^\circ$ . However,

for angles  $40^\circ \leq \alpha \leq 60^\circ$  the boron/epoxy composite loses its resistance qualities with respect to the other two graphite/epoxy and glass/epoxy composites. It is noted that the properties of these latter composites allow a better attenuation of the parameter  $K_I$  compared to the boron/epoxy composite for angles of orientation of the fibers greater than  $60^\circ$ .

The results obtained numerically by the element method

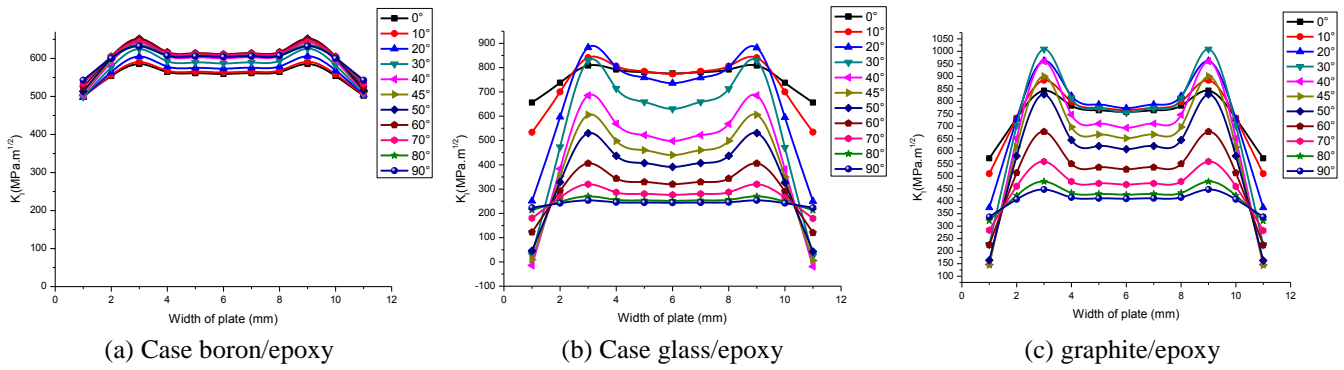


Fig. 10 Variation of the  $K_I$  factor as a function of delamination with of the three composite and for various angles  $\alpha$  ( $+\alpha/-\alpha$ ) (a: boron/epoxy, b: glass/epoxy and c: graphite/epoxy.)

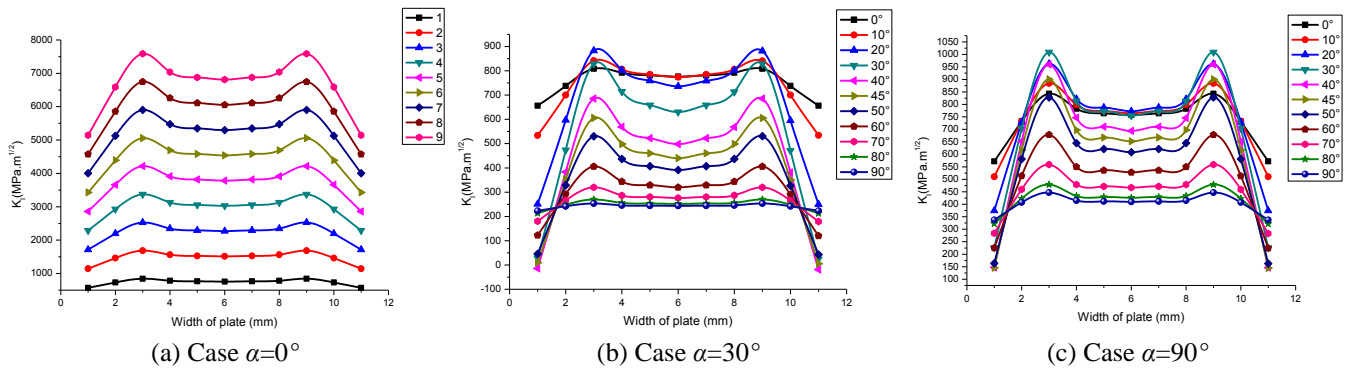


Fig. 11 Variation of the  $K_I$  factor as a function of the applied load of the glass/epoxy composite and for different angles  $\alpha$  ( $+\alpha/-\alpha$ ) (a:  $\alpha=0^\circ$ , b:  $\alpha=30^\circ$  and c:  $\alpha=90^\circ$ )

show the variation of the stress intensity factor as a function of the width of the delamination for two angles of orientation of the plies of the graphite/epoxy and glass/epoxy laminate composite ( $\alpha=0^\circ$  and  $\alpha=20^\circ$ ). It is noted that the two curves determined for these two angles are totally confounded, that is to say that the properties of these two composites have no influence on the propagation of delamination.

It is observed that for the two angles of orientation of the fibers  $\alpha=30^\circ$  and  $\alpha=40^\circ$ , the stress intensity factor of the glass/epoxy composite is higher than that of the graphite/epoxy composite in the middle of the separation width and in the vicinity close to the free end of the composite plate but it remains constant at the free edges of the two composites. The difference in the stress intensity factors of glass/epoxy and graphite/epoxy composites increases with increasing fiber orientation angle  $\alpha=50^\circ$  and  $\alpha=60^\circ$  in the middle of the delamination width and in the vicinity close to the free ends, however the phenomenon is reversed at the free ends of the composites. For angles ranging from  $70^\circ$  to  $90^\circ$  the difference between the stress intensity factors of glass/epoxy and graphite/epoxy composites is almost constant over the entire delamination width whose level of the SIF  $K_I$  of the glass/Epoxy is always higher than that of the graphite/epoxy composite.

The mechanical properties of the graphite/epoxy composite increase the mechanical strength of the composite plate and improve its mechanical strength during operation, in particular for an angle of orientation of the

folds equal to  $90^\circ$ .

### 3.2.7 Influence of the delamination length on the $K_I$ factor for different orientations of the fibers

Fig. 10(a), 10(b) and 10(c) show the variation of the SIF  $K_I$  as a function of the width of the detachment of the three composites for different orientation angles of the fibers. These graphs confirm the result obtained in Fig. 9.

### 3.2.8 Influence of the applied load on the $K_I$ factor for different orientations of the fibers

Fig. 11(a), 11(b) and 11(c) show the variation of the FIC KI as a function of the force applied to the glass/epoxy composite plate for the three orientation angles of the respective fibers  $0^\circ$ ,  $30^\circ$  and  $90^\circ$ . It can be seen that whatever the angle of the folds  $+\alpha/-\alpha$  the SIF  $K_I$  increases with the increase of the applied load. When the fibers are oriented at an angle  $\alpha=0^\circ$ , the maximum load leads to the damage of the composite in the vicinity close to the free ends.

On the other hand, the orientation of the folds at an angle  $\alpha=90^\circ$  leads to a significant reduction of the SIF  $K_I$ , which slows down the delamination propagation even when the composite is subjected to high intensity charges. The orientation of the folds at an angle  $\alpha=30^\circ$  of the glass/epoxy composite stressed at intense loads leads to a SIF  $K_I$  which exceeds the toughness of the composite material, which promotes delamination and weakens the mechanical strength of the laminated composite.

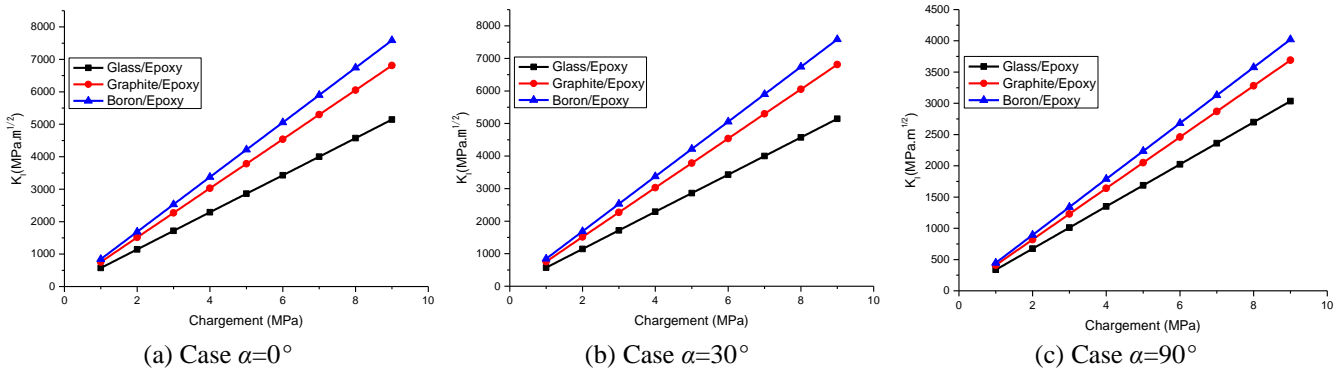


Fig. 12 Variation of the  $K_I$  factor as a function of the applied load of the three composites and for different angles  $\alpha$  ( $+\alpha/-\alpha$ ) (a:  $\alpha=0^\circ$ , b:  $\alpha=30^\circ$  and c:  $\alpha=90^\circ$ )

### 3.2.9 Influence of the applied load on the $K_I$ factor for different materials

Fig. 12 illustrates the variation of the SIF  $K_I$  as a function of the force applied to the glass/epoxy, graphite/epoxy and glass/epoxy composite plate for the three angles of orientation of the fibers respectively  $0^\circ$ ,  $30^\circ$  and  $90^\circ$ . It is noted that the SIF varies in proportion to the load applied to the glass/epoxy composite. The curve of the stress intensity factor is a straight line.

## 4. Conclusions

This numerical analysis by the finite element methods allows us to draw the following conclusions:

The propagation of pure mode I delamination depends on the type of stress applied to the laminated composite. In our study, mode I was decoupled of the two modes II and III.

The delamination of the composite begins at the zone which is in the vicinity close to the two free ends of the laminated composite.

The peak of the stress intensity factor is more intense for the angles of orientations of the fibers ranging from  $0^\circ$  to  $50^\circ$  and its intensity decreases with the increase of the angle  $\alpha$  in the interval  $[60^\circ, 90^\circ]$ .

The two orientations of the fibers at  $80^\circ$  and  $90^\circ$  angles result in a small peak of the SIF  $K_I$ .

The increase of the detachment surface leads to an increase of the peak of the SIF  $K_I$ .

Regardless of the angle  $\alpha$  and the length  $d$ , the  $K_I/K_{IC}$  ratio is almost constant in the middle over a distance of 40% of the delamination width and the level of the stress intensity factor  $K_I$  strongly depends on the angle fiber orientation and delamination length. The parameter  $K_I$  reaches a minimum value for an angle of the fibers  $\alpha=90^\circ$ .

At the free edges of the composite plate, the  $K_I/K_{IC}$  ratio depends on the angle  $\alpha$  of the layers of the laminated composite and the detachment surface and reaches minimum values in this area and even negative values. At the free edges of the composite, it can be seen that whatever the angle  $\alpha$  and the length  $d$  of the detachment surface. Therefore the propagation of the delamination is either slowed down or totally stopped. The angle of the fibers

equal to  $40^\circ$  leads to a decrease in the stress intensity factor and the variation of the parameter  $K_I$  is not proportional to the detachment length.

The mechanical properties of the graphite/epoxy composite increase the mechanical strength of the composite plate and improve its mechanical strength during operation, in particular for an angle of orientation of the folds equal to  $90^\circ$ . Compared with graphite/epoxy and glass/epoxy composites, the boron/epoxy laminate composite reduces more the SIF  $K_I$  in the middle of the plate for fiber angles  $0^\circ \leq \alpha \leq 30^\circ$ . However, for corners the boron/epoxy composite loses its qualities of resistance.

Whatever the angle of the folds  $+\alpha/-\alpha$  the SIF  $K_I$  grows proportionally with the increase of the applied load.

## References

- Anderson, T.L. (2005), *Fracture Mechanics-Fundamentals and Applications*, 3rd Edition, CRC Press.
- Haneef, M., Sa, R. and Ali, M.M. (2011), "Studies on delaminating effects on stress development in composite structures", *Proceedings of the World Congress on Engineering* Vol. III WCE, July, London, U.K.
- Jayatilake, I.N., Karunasena, W. and Lokuge, W. (2016), "Finite element based dynamic analysis of multilayer fibre composite sandwich plates with interlayer delaminations. *Indunil*", *Adv. Aircraft Spacecraft Sci.*, **3**(1), 15-28.
- Kutlu, Z. and Chang, F.K. (1992), "Modeling compression failure of laminated composites containing multiple through-the-width delaminations", *J. Compos. Mater.*, **26**(3), 350e86.
- Li, D.H., Liu, Y. and Zhang, X. (2015), "An extended Layerwise method for composite laminated beams with multiple delaminations and matrix cracks", *Int. J. Numer. Meth. Eng.*, **101**, 407e34.
- Liu, L., Zhang, J., Wang, H. and Guan, Z. (2015), "Mechanical behavior of the composite curved laminates in practical applications". *Steel Compos. Struct.*, **19**(5), 1095-1113.
- Liu, Y. and Shu, D.W. (2015), "Effects of edge crack on the vibration characteristics of delaminated beams", *Struct. Eng. Mech.*, **53**(4), 767-780.
- Maimi, P., Camanho, P.P., Mayugo, J.A. and Turon, A. (2011), "Matrix cracking and delamination in laminated composites", Part I: Ply constitutive law, first ply failure and onset of delamination", *Mech. Mater.*, **43**, 169-185.
- Product Dassault Systèmes Simulia Corp (2012), ABAQUS Standard Version 6.12, Providence, RI, USA.

- Rooke, D.P. and Cartwright, D.J. (1976), "Compendium of stress intensity factors", HMSO Ministry of Defence, Procurement Executive.
- Seo, D.C. and Lee, J.J. (2002), "Fatigue crack growth behavior of cracked aluminum plate repaired with composite patch", *Compos. Struct.*, **57**, 323-330.
- Short, G.J., Guild, F.J. and Pavier, M.J. (2001), "The effect of delamination geometry on the compressive failure of composite laminates", *Compos. Sci. Technol.*, **61**, 2075e86.
- Suemasu, H., Sasaki, W., Ishikawa, T. and Aoki, Y. (2008), "A numerical study on compressive behavior of composite plates with multiple circular delaminations considering delamination propagation", *Compos. Sci. Technol.*, **68**, 2562-2567.
- Tada, H., Paris, P. and Irwin, G. (2000), *The Stress Analysis of Cracks Handbook*, 3rd Edition, ASME Press.
- Todo, M. and Jar, P.Y. (1998), "Study of mode-I interlaminar crack growth in DCB specimens of fibre-reinforced composites", *Compos. Sci. Technol.*, **58**, 105-118.
- Wang, X.W., Lezica, I.P., Harris, J.M., Guild, F.J. and Pavier, M.J. (2005), "Compressive failure of composite laminates containing multiple delaminations", *Compos. Sci. Technol.*, **65**, 191e200.
- Zhao, L., Gong, Y., Zhang, J., Chen, Y. and Fei, B. (2014), "Simulation of delamination growth in multidirectional laminates under mode I and mixed mode I/II loadings using cohesive elements", *Compos. Struct.*, **116**(1), 509-522.